Reactive Oxygen Species-Triggered Trophoblast Apoptosis Is Initiated by Endoplasmic Reticulum Stress via Activation of Caspase-12, CHOP, and the JNK Pathway in *Toxoplasma gondii* Infection in Mice

Xiucai Xu,[a,b] Tingting Liu,[a] Aimei Zhang,[a,b] Xingxing Huo,[a] Qingli Luo,[a] Zhaowu Chen,[a] Li Yu,[a] Qing Li,[b] Lili Liu,[a,c] Zhao-rong Lun,[d] and Jilong Shen[a]

Anhui Provincial Laboratories of Pathogen Biology and Zoonoses, Department of Microbiology and Parasitology, Anhui Medical University, Hefei, China[a]; Central Laboratory of Affiliated Provincial Hospital of Anhui Medical University, Hefei, China[b]; Department of Laboratory Diagnosis, the Fourth Affiliated Hospital of Anhui Medical University, Hefei, China[c]; and Center for Parasitic Organisms, State Key Laboratory of Biocontrol, School of Life Sciences and Key Laboratory of Tropical Diseases and Control of the Ministry of Education, Zhongshan Medical School, Sun Yat-Sen University, Guangzhou, China[d]

Toxoplasma gondii infection in pregnant women may result in abortion or in fetal teratogenesis; however, the underlying mechanisms are still unclear. In this paper, based on a murine model, we showed that maternal infection with RH strain *T. gondii* tachyzoites induced elevated production of reactive oxygen species (ROS), local oxidative stress, and subsequent apoptosis of placental trophoblasts. PCR array analysis of 84 oxidative stress-related genes demonstrated that 27 genes were upregulated at least 2-fold and that 9 genes were downregulated at least 2-fold in the *T. gondii* infection group compared with levels in the control group. The expression of NADPH oxidase 1 (Nox1) and glutathione peroxidase 6 (Gpx6) increased significantly, about 25-fold. The levels of malondialdehyde (MDA) and 8-hydroxydeoxyguanosine (8-OHdG) increased significantly with *T. gondii* infection, and levels of glutathione (GSH) decreased rapidly. *T. gondii* infection increased the early expression of endoplasmic reticulum stress (ERS) markers, followed by cleavage of caspase-12, activation of ASK1/JNK, and increased apoptosis of trophoblasts, both *in vivo* and *in vitro*. The apoptosis of trophoblasts, the activation of caspase-12 and the ASK1/JNK pathway, and the production of peroxides were dramatically inhibited by pretreatment with *N*-acetylcysteine (NAC). The upregulation of Nox1 was contact dependent and preceded the increase in levels of ERS markers and the activation of the proapoptosis cascade. Thus, we concluded that apoptosis in placental trophoblasts was initiated predominantly by ROS-mediated ERS via activation of caspase-12, CHOP, and the JNK pathway in acute *T. gondii* infection. Elevated ROS production is the central event in *T. gondii*-induced apoptosis of placental trophoblasts.

Toxoplasma gondii is an obligate intracellular protozoan parasite that infects all warm-blooded animals, including approximately 30% of the human population worldwide (42). Infection is normally asymptomatic, but congenital fetal toxoplasmosis may result in abortion, stillbirth, severe mental retardation, and retinal or neurologic damage later in life. Although birth defects caused by *T. gondii* could be attributed to structural damage (49), endocrine disorders (16), and increased cell apoptosis of placental tissue (1), the exact mechanisms and key events underlying congenital toxoplasmosis remain unclear. *T. gondii* has a fascinating dual involvement in host cell apoptosis. Some previous studies demonstrated that *T. gondii*-infected cells became relatively resistant to some apoptotic stimuli (34). On the other hand, it has been observed that *T. gondii* infection can induce apoptosis, as with CD4+ splenocytes during acute infection of mice with *T. gondii* (23). High levels of apoptosis and an increased mortality rate have been proven to be associated with *T. gondii* infection with high-virulence strains (15). In contrast, in chronic toxoplasma encephalitis, only a few apoptotic cells were observed. Therefore, the initiation and the degree of cell apoptosis may play crucial roles in the pathogenesis and outcomes of toxoplasmosis, but the exact mechanisms and key events underlying congenital toxoplasmosis remain unclear.

The endoplasmic reticulum (ER) is the primary intracellular organelle for proper protein synthesis, folding, and assembly. The accumulation of unfolded or misfolded proteins in the lumen of the ER, which induces an adaptive program called the unfolded protein response (UPR), leads to ER stress (ERS). Increasing evidence shows that ERS plays a key role in the regulation of apoptosis caused by a variety of toxic insults, including reactive oxygen species (ROS), chemicals, and heavy metals. Oxidative stress is described as an imbalance between ROS generation and antioxidant capacity, and such stress triggers apoptosis through a variety of signaling pathways, such as ERS response and the activation of the ASK1/JNK pathway (21). These pathological processes can be simultaneously observed in some diseases, such as diabetes, cadmium poisoning, and neurodegenerative diseases (24, 30, 45). Additionally, there is growing evidence that oxidative stress plays an important role in infection-induced apoptosis (11, 31, 41).

Generally, pregnancy is a state of mild oxidative stress arising from increased placental mitochondrial activity and ROS production for maternal and fetal metabolism. In the first trimester, establishment of blood flow into the intervillous space results in a burst of oxidative stress (20). The placenta is subjected to hypoxia

and then hypoxia/reoxygenation; the inability to mount an effective antioxidant defense contributes to early pregnancy loss. In late gestation, increased oxidative stress is observed in pregnancies complicated by diabetes, intrauterine growth restriction, and preeclampsia in association with escalated trophoblast apoptosis (5, 48). Previous studies revealed that *T. gondii* infection can lead to oxidative stress and immune suppression in blood donors (12). Th2 immune bias can be seen in the normal maternal-fetal interface, which is unfavorable to the elimination of pathogens (3) and enhances susceptibility to toxoplasmosis (35). Thus, *T. gondii* infection or the reactivation of latent infection during pregnancy will increase oxidative stress in the placenta, contribute to cell apoptosis and placenta damage, and, finally, lead to more serious outcomes than would be seen during the normal physiological state. The relationship between oxidative stress and cell apoptosis in gestation-related disease has been reported. Wang and colleagues demonstrated that lipopolysaccharide (LPS) could induce oxidative stress in several tissues, leading to preterm labor in mice (44). Some studies discovered that trophoblasts could be productively infected by a virulent strain of *T. gondii*, and that uninfected, but not infected, cells undergo apoptosis (1, 31, 39), which indicated that *T. gondii*-induced apoptosis was not due to a direct action of the parasite at the maternofetal interface.

Therefore, we hypothesized that *T. gondii* infection would significantly increase ROS generation and subsequent trophoblast apoptosis at the maternal-fetal interface. In the present study, we explored the role of ROS and the downstream activation by ROS in the mechanisms of placental trophoblast apoptosis induced by *T. gondii* infection. To this aim, we investigated the involved oxidative and antioxidative molecules by PCR array, the parasite burden of placenta tissues and blood samples by real-time PCR, the trophoblast apoptosis index by terminal deoxynucleotidyltransferase-mediated dUTP-biotin nick end labeling (TUNEL) and flow cytometry (FCM), and the local oxidative stress by examining increased malondialdehyde (MDA), 8-hydroxydeoxyguanosine (8-OHdG), and reduced glutathione (GSH) levels of placental tissues. Simultaneously, ERS, p38, and JNK pathways in placental tissues from mouse congenital toxoplasmosis models and *in vitro* primary cultured trophoblasts in a transwell coculture system were observed by real-time reverse transcription-PCR (RT-PCR) and Western blotting.

MATERIALS AND METHODS

***In vivo* passage of *T. gondii* tachyzoites.** Tachyzoites of the highly virulent RH strain of *T. gondii* were maintained in BALB/c mice by intraperitoneal passage at 72-h intervals. Parasites were obtained from mouse peritoneal exudates, washed twice (at $1,000 \times g$ for 15 min) in sterile phosphate-buffered saline (PBS; pH 7.2) and maintained by serial passage in human foreskin fibroblasts (HFF) for further infection experiments *in vitro* and *in vivo*.

Mouse models and treatment. All procedures were in strict accordance with the Chinese National Institute of Health Guide for the Care and Use of Laboratory Animals and approved by the Animal Care and Use Committee of Anhui Medical University. Efforts were made to minimize the number of animals used and their suffering. Six- to 8-week-old ICR mice (body weight, 20 to 22 g), obtained from the Animal Department of Anhui Medical University, were maintained on a 12-h light/dark cycle from 8:00 a.m. to 8:00 p.m. in a controlled, specific-pathogen-free environment (temperature, $20° \pm 1°C$). Animals were housed in plastic cages with free access to food and water. The mice were acclimatized for at least 1 week before being mated. For mating purposes, four females were

housed overnight with two males at 9:00 p.m. Females were checked by 7:00 a.m. the next morning, and the presence of a vaginal plug or sperm in the vaginal smear was considered as marking gestational day 0 (GD0). Pregnant females were maintained in the animal care facility until they were infused with tachyzoites or saline. On GD7, pregnant females were randomly divided into the following three groups: *T. gondii* infection, *N*-acetylcysteine (NAC) pretreatment plus *T. gondii* infection, and control. Mice were maintained in the animal care facility until they were treated. On GD8 and GD9, mice in the NAC pretreatment group were infused with NAC (100 mg/kg of body weight). On GD8, each mouse in the *T. gondii* infection group and NAC pretreatment group was injected intraperitoneally with 200 tachyzoites in 0.1 ml of 0.9% sterile saline solution. In the control group, the mice were exposed to only 0.9% sterile saline solution. Mice were killed by cervical dislocation on gestational days 10, 12, 14, 16, and 18. Placentas were carefully dissected and, after their weights were recorded, processed into cell suspension or fixed in Bouins fluid for immunohistochemical analysis; samples were then snap frozen in liquid nitrogen for other types of analysis.

Analysis of oxidative stress and antioxidant defense molecules by PCR array. Tissue samples were homogenized in 1 ml of TRIzol reagent per 50 to 100 mg of tissue using a power homogenizer. RNA isolation was performed according to the conventional method, and the yield and quality of RNA were assessed by spectrophotometer and gel electrophoresis. Mouse Oxidative Stress and Antioxidant Defense RT^2 Profiler PCR Array kits were obtained from SABioscience Company (Frederick, MD). First-strand cDNA synthesis and real-time PCR were conducted based on the manufacturer's instructions. The relative gene expression was determined by ABI 7500 real-time detection system software (SDS, version 2.05) using an adaptive baseline to determine the threshold cycle (C_T). The data were analyzed by the $\Delta\Delta C_T$ method according to the manufacturer's manual. Quality control was performed using genomic DNA and reverse transcription- and positive-PCR controls. The data were normalized to the housekeeping gene β-actin. Changes in gene expression were represented as fold increase/decrease. Genes were considered to be upregulated or downregulated if changes in expression levels were ≥2.0-fold or ≤2.0-fold, respectively.

Primary trophoblast culture and experimental infection. The placentas (GD12) were obtained from normal pregnant mice. Cells were isolated according to the method of mouse trophoblast isolation described elsewhere (2), with appropriate modifications. Briefly, the placentas were carefully cut into pieces with scissors and digested by trypsin and collagenase I to obtain primary trophoblast cells. Detached trophoblasts were washed in Iscove's modified Dulbecco's medium (IMDM; Gibco) supplemented with 10% fetal bovine serum (FBS; Gibco) and were purified over a Percoll gradient. To decrease residual macrophage and fibroblast cell contamination, the cells were seeded at 10^5/microwell/100 μl of 10% FBS in 24-well tissue culture plates (product number 3527; Corning) and incubated for 4 h at 37°C in a 5% CO_2 humidified atmosphere; the nonadherent cells and debris were removed by washing the plates with prewarmed IMDM. Cell passage was performed several times by 0.25% trypsin digestion for 2 min at 37°C to minimize the contamination of the macrophage. The characterization of the trophoblast cell population was carried out through positive immunolocalization of the cytokeratin-7 and negative reactivity to vimentin (18). Anti-cytokeratin-7–fluorescein isothiocyanate (FITC), anti-vimentin-horseradish peroxidase (HRP; Huayi Biotechnology Co., China), and anti-F4/80-FITC (eBioscience, San Diego, CA) were used to identify the purity and phenotype of cells by FCM analysis and immunohistochemical and immunofluorescent staining. Cytokeratin-7-positive cells were counted randomly, and results are expressed as a percentage of the total cell number. Experimental infection was performed with a transwell system using cell culture plates with a 0.4-μm-pore-size filter (Falcon, Franklin Lakes, NJ). Cell culture medium and reagents were obtained from Invitrogen. Freshly prepared parasites (1×10^6) were added to the upper well, which contained a monolayer of placental cells (1×10^6). The placental trophoblasts (1×10^6) in the lower

TABLE 1 Sequences of oligonucleotide primers used for real-time PCR

Target	Forward primer (5′–3′)	Reverse primer (5′–3′)	Product size (bp)
GRP78	ATCAGGGCAACCGCATCA	CGCATCGCCAATCAGACG	71
GRP94	GGTGTTGTGGATTCCGATG	AGAAGTTTAGCAAGCCGTGTT	227
CHOP	CAGCGACAGAGCCAGAATAAC	ACCGTCTCCAAGGTGAAAGG	148
XBP1	GAACCAGGAGTTAAGAACACG	AGGCAACAGTGTCAGAGTCC	205
Caspase-12	GTGATGGAGAAGGAGGGACGAACA	ACCAGGAATGTGCTGTCTGAGGA	235
ATF4	TTGCCCCCTTTACATTCTTG	GGAATGCTCTGGAGTGGAAG	71
Nox1	AGCAGCAGGGGACTGGACAC	GCCACTTCATACTGGAAAACATC	126
Gpx6	CTGGTGGGACCTGATGGA	TGGTGACCGAGTGGAACA	150
Gpx1	CCAGGAGAATGGCAAGAATGAAGA	GCAGGAAGGTAAAGAGCGGGTGA	140
GAPDH	CAACTTTGGCATTGTGGAAGG	ACACATTGGGGGTAGGAACAC	224

wells remained uninfected and were cocultured with infected cells from the upper well on a 12-well plate at 37°C for the time intervals indicated in the figure legends before being subjected to the apoptosis assay by TUNEL and FCM, as well as to the real-time RT-PCR and immunoblotting for the detection of ERS or other proapoptotic pathways.

Detection of apoptosis by annexin V/PI and flow cytometry. An annexin V-enhanced green fluorescent protein (EGFP)/propidium iodide (PI) kit for an apoptosis assay was purchased from BestBio (Shanghai, China). Cell suspensions from placental tissues or primary cultured trophoblasts were harvested and washed twice with PBS and resuspended in 400 μl of annexin V binding buffer (10 mM HEPES, 0.14 M NaCl, and 0.25 mM CaCl$_2$). Then, 5 μl of EGFP-conjugated annexin V was added and incubated at room temperature for 15 min in the dark with gentle vortexing. Next, 10 μl of propidium iodide was added and incubated at room temperature for 5 min in the dark. Finally, 400 μl of 1× binding buffer was added to each tube. The cells were analyzed on a Coulter Epics Altra HyPerSort system (Beckman Coulter, FL), and the data were analyzed using EXPO32 Multicomp software. Early and late apoptosis were analyzed to better observe the effect of *T. gondii* infection or NAC treatment on apoptosis signal. Annexin V-positive, PI-negative (annexin V$^+$ PI$^-$) cells are early apoptotic cells, and annexin V$^+$, PI-positive (PI$^+$) cells are late apoptotic cells (14).

Detection of apoptotic cells *in situ* using TUNEL. Placental tissues embedded in paraffin were cut into 5-μm-thick sections using a microtome. For TUNEL assays, these sections were immersed in xylene in a coupling jar to remove paraffin and rehydrated in graded ethanol solutions. DNA fragmentation was detected using a TUNEL kit (Roche Diagnostics GmbH, Mannheim, Germany) according to the manufacturer's instructions, with some modifications. Apoptotic cells were directly detected as green using fluorescence microscopy (Olympus IX51; Olympus, Tokyo, Japan). Images were captured with a charge-coupled-device (CCD) camera and QCapture Pro 6 software (QImaging, Burnaby, BC, Canada) for real-time image preview and capture. To assess the extent of apoptosis, the number of TUNEL-stained nuclei was counted by two investigators who were blinded with regard to the treatments in four randomly selected microscopic fields at a ×200 magnification per section. Data obtained from two sections per animal were then averaged. Values are presented as the mean ± standard deviation (SD).

Measurement of MDA, GSH, and 8-OHdG in placenta homogenates. Frozen placental tissues were thawed, weighed, and homogenized in phosphate-buffered saline (pH 7.4). Homogenates were centrifuged (at 2,000 × *g* for 10 min at 4°C), and the supernatant was used immediately for assays of MDA, GSH, and 8-OHdG.

The total protein concentration from placental tissues or cultured primary cells was determined using a bicinchoninic acid protein assay kit with an absorption band of 570 nm (Pierce, Rockford, IL). Commercial assay kits used to determine lipid peroxidation (MDA) and GSH were produced by the Jiancheng Institute of Biotechnology (Nanjing, China); the kit for 8-OHdG was obtained from Cell Biolabs (San Diego, CA). MDA, GSH, and 8-OHdG were all strictly determined following the in-

structions of the commercial kits. The formation of MDA, a substance produced during lipid peroxidation, was determined by the thiobarbituric acid method. MDA level is expressed as micromoles per gram of protein.

GSH analysis was performed as described previously (40). Briefly, after centrifugation at 2,000 × *g* for 10 min, 0.5 ml of supernatant was added to 2 ml of 0.3 mol/liter Na$_2$HPO$_4$ · 2H$_2$O solution. A 0.2-ml solution of dithiobisnitrobenzoate (0.4 mg/ml in 1% sodium citrate) was added, and the absorbance at 412 nm was measured immediately after mixing. Results are expressed as micromoles per gram of protein.

The level of 8-OHdG was measured according to the protocol of the enzyme-linked immunosorbent assay (ELISA) kit. The unknown 8-OHdG samples or 8-OHdG standards were first added to an 8-OHdG/bovine serum albumin (BSA) conjugate-preabsorbed ELISA plate. After a brief incubation, an anti-8-OHdG monoclonal antibody (Ab) was added, followed by an HRP-conjugated secondary antibody. The 8-OHdG content in unknown samples was determined by comparison with a predetermined 8-OHdG standard curve.

Detection of tachyzoite burden and oxidative stress-associated molecules by real-time PCR. The extraction and purification of *T. gondii* DNA from placenta tissues or blood samples were performed according to the manufacturer's instructions (QIAamp DNA Minikit, Qiagen, Germany). The tachyzoite burden was assessed by using a commercial kit (DaAn, China). Total RNA was isolated using TRIzol reagent (Invitrogen, CA) following the instructions of the manufacturer. The cDNA was synthesized from total RNA using Superscript II reverse transcriptase and random primers (Invitrogen). To investigate apoptosis-associated or oxidative stress-associated molecules, quantitative real-time RT-PCR was performed using specific primer sets (Shenggong, Shanghai, China) and a single-tube SYBR green kit (TaKaRa, Tokyo, Japan) with an ABI 7500 real-time PCR system (Applied Biosystems, SA). The primers used for PCR are listed in Table 1. Only experiments in which a distinct single peak was observed with a melting temperature different from that of the no-template control were analyzed. The mRNA fold induction values were calculated by the following equations: $\Delta C_T = \Delta C_{T(\text{target})} - \Delta C_{T(\text{GAPDH})}$; $\Delta\Delta C_T = \Delta C_{T(\text{infected})} - \Delta C_{T(\text{control})}$; mRNA fold change = $2^{-\Delta\Delta C_T}$ (GAPDH is glyceraldehyde-3-phosphate dehydrogenase). Experiments were performed in triplicate, and data are expressed as mean ± SD.

Immunoblotting. Placental tissues were dissected and homogenized in ice-cold lysis buffer (25 mM HEPES, 1.5% Triton X-100, 0.1% sodium dodecyl sulfate [SDS], 0.5 M NaCl, 5 mM EDTA, and 0.1 mM sodium deoxycholate) containing a protease inhibitor cocktail (Roche, Boehringer Mannheim, Germany) and phosphatase inhibitor (Phosphatase Inhibitor Cocktail Set II; Merck, Germany). Primary cultured trophoblasts were directly treated with 100 μl of lysis buffer. Total cell lysates were subjected to SDS-PAGE. Separated proteins were transferred to nitrocellulose membranes (Millipore Corp., Billerica, MA); the membranes were blocked with 5% skim milk, and conventional immunoblotting was performed using several Abs. Chemiluminescence was detected using an ECL kit (SuperSignal West Pico; Thermo Scientific). Anti-β-actin
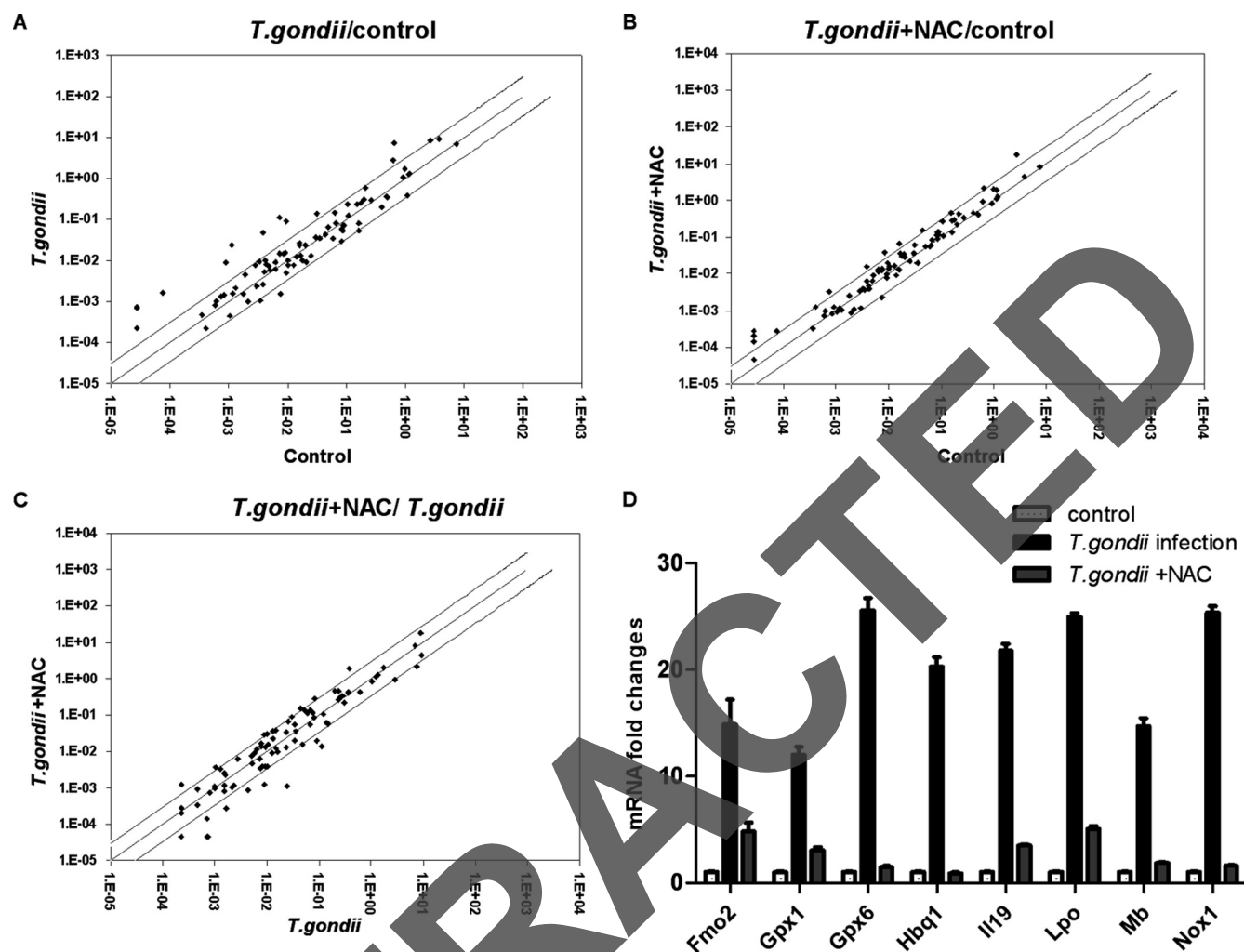
FIG 1 Oxidative response-related gene expression profiles in three groups. Differences between two groups were considered significant given at least a 2-fold variation. (A, B, and C) The cutoff levels are shown with black lines (the expression levels of some genes were similar and nearly overlapped in this graph). The expression of the specific gene is higher in this group the black dot near to, compared to that in the other group. (D) Eight genes differed more than 10-fold between the control group and the *T. gondii* infection group. The experiments were repeated three times. Fmo2, flavin containing monooxygenase 2; Hbq1, hemoglobin, theta 1; Il19, interleukin-19; Lpo, lactoperoxidase; Mb, myoglobin.

antibody and the horseradish peroxidase-conjugated secondary antibody to rabbit were obtained from Santa Cruz Biotechnology (Santa Cruz, CA). Anti-C/EBP homologous protein (CHOP) was purchased from Abcam, Ltd. (Hong Kong). Anti-glucose-regulated protein 78 (GRP78), anti-phospho-JNK (Thr183/Tyr185), anti-phospho-p38 mitogen-activated protein kinase ([MAPK] Tyr182), anti-p38 MAPK, anti-caspase-12, and anti-phospho-ASK1 were obtained from Cell Signaling Technology (Danvers, MA). The results were analyzed using ImageJ, version 1.44, software.

Statistical analysis. All data are expressed as mean ± SD. Differences between groups were assessed by one-way analysis of variance (ANOVA) and the Student Newman Keuls (SNK) multiple comparison posttest or Student's *t* test. Differences were considered statistically significant at a *P* value of <0.05.

RESULTS

***T. gondii* infection alters oxidative-response-related gene expression profile in placental tissues.** To clarify whether *T. gondii* infection would result in increased ROS production and oxidative stress, we investigated the gene expression profile of placenta tis-

sues from GD12 mice in the *T. gondii* infection group with a 96-well RT^2 Profiler PCR Array containing 84 key genes related to oxidative stress. This mouse PCR array includes antioxidants involved in ROS metabolism and relevant oxygen transporter genes. Meanwhile, the results were compared with ones of the control group and NAC pretreatment group. RT-PCR was performed to detect expression of several representative genes, showing the consistency of the assays (data not shown).

Twenty-seven genes were upregulated at least 2-fold, and nine were downregulated at least 2-fold in the *T. gondii* infection group compared with expression in the control group (Fig. 1A). Eight genes differed more than 10-fold between the control group and *T. gondii* infection group (Fig. 1D). For example, two key antioxidant enzymes, Gpx6 and Gpx1, adaptively increased in the infected group versus the control group by about 25 and 12 times, respectively. As the main source of ROS production, NADPH oxidase 1 (Nox1) also increased about 25 times as a result of *T. gondii* infection, which could contribute to excessive production of ROS.
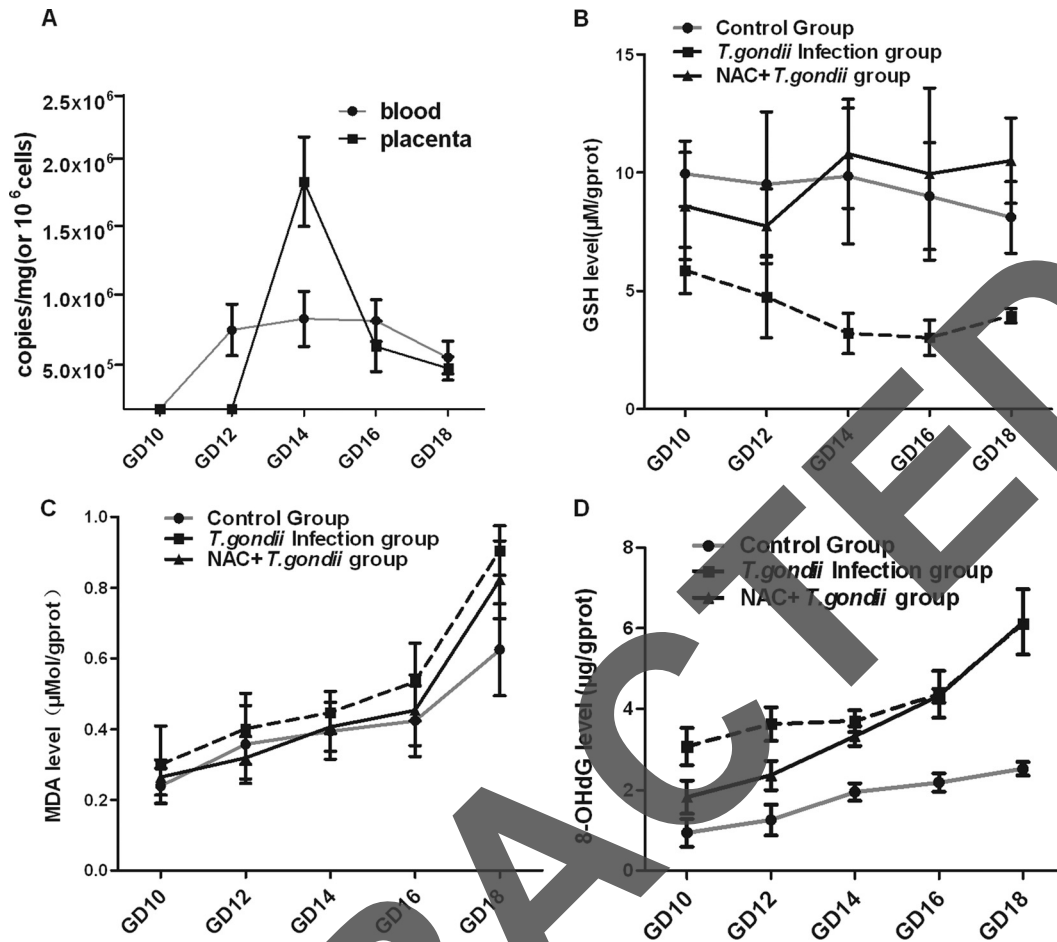
FIG 2 Acute *T. gondii* infection-induced oxidative stress response and products of peroxidation. (A) Three mice of each gestation day and three placentas or blood samples from each pregnant mouse were picked for analysis by real-time PCR. Fifty milligrams of tissue or 10^7 nucleated cells were used for DNA extraction. Parasite burden is presented as copies per mg (placenta) or 10^6 cells (blood). Analyses of GSH (B), MDA (C), and 8-OHdG (D) levels were conducted per the manufacturer's instructions. The results of each gestation day are shown as mean ± SD ($n = 6$), and results were compared by one-way ANOVA; the SNK multiple comparison posttest was used to compare levels of various gestational days.

The above-mentioned genes were detected at almost the levels seen in the control group when the infected mice were pretreated with NAC (Fig. 1B, C, and D).

T. gondii infection enhances oxidative stress of the placenta and leads to peroxidation of lipids and DNA. A burst of oxidative response occurred in the placental tissues of subjects infected with *T. gondii*. To discover the origin of the increased oxidative stress, the placenta tissues and blood samples of pregnant mice from the *T. gondii* infection group were checked for assessment of parasite burden. Next, we evaluated local oxidative stress and placenta structural damage through analysis of GSH, MDA, and 8-OHdG levels in placenta tissue homogenates. By quantitative PCR analysis, *T. gondii* was not detectable in the placentas of GD10 and GD12. A dramatic increase in parasite load, however, was found in those of GD14. Additionally, our data also showed that the parasitemia occurred and GSH level of placentas decreased before GD12 in the *T. gondii* infection group (Fig. 2A and B, respectively). Additionally, MDA and 8-OHdG were elevated to different degrees after *T. gondii* infection (Fig. 2C and D). NAC could weaken the oxidative response, further protecting the infected placenta from serious damage (Fig. 2).

Isolated trophoblasts were identified through a variety of immunological and morphological means. Primary trophoblast cells appeared as irregular polygons or round (Fig. 3A, left) and were confirmed by immunostaining for cytokeratin-7, an epithelial cell marker. Although about 5.1% of cultured cells were macrophages, by analysis of FCM (Fig. 3B), most cells (90.5% ± 3.5%) showed positive staining for cytokeratin-7 (Fig. 3C). Additionally, positive reactivity to vimentin was not noted (Fig. 3A, the upper right), which indicated that the cell cultures did not contain large numbers of contaminating fibroblast or endothelial cells.

T. gondii induces apoptosis of trophoblasts in placental tissues *in vivo* and of primary cultured cells in *vitro*. To estimate the effects of local oxidative stress and peroxidation damage on placental trophoblasts, trophoblast apoptosis was analyzed by FCM. We found that the apoptosis levels in the infection group increased with the duration of infection (Fig. 4A, top), but no significant difference in apoptosis across gestation days was found in the control group (Fig. 4A, bottom). According to the apoptosis index from the control and *T. gondii* infection groups, total, early, and late apoptosis were significantly enhanced in the *T. gondii* infection group (Fig. 4B). Additionally, the apoptosis index of
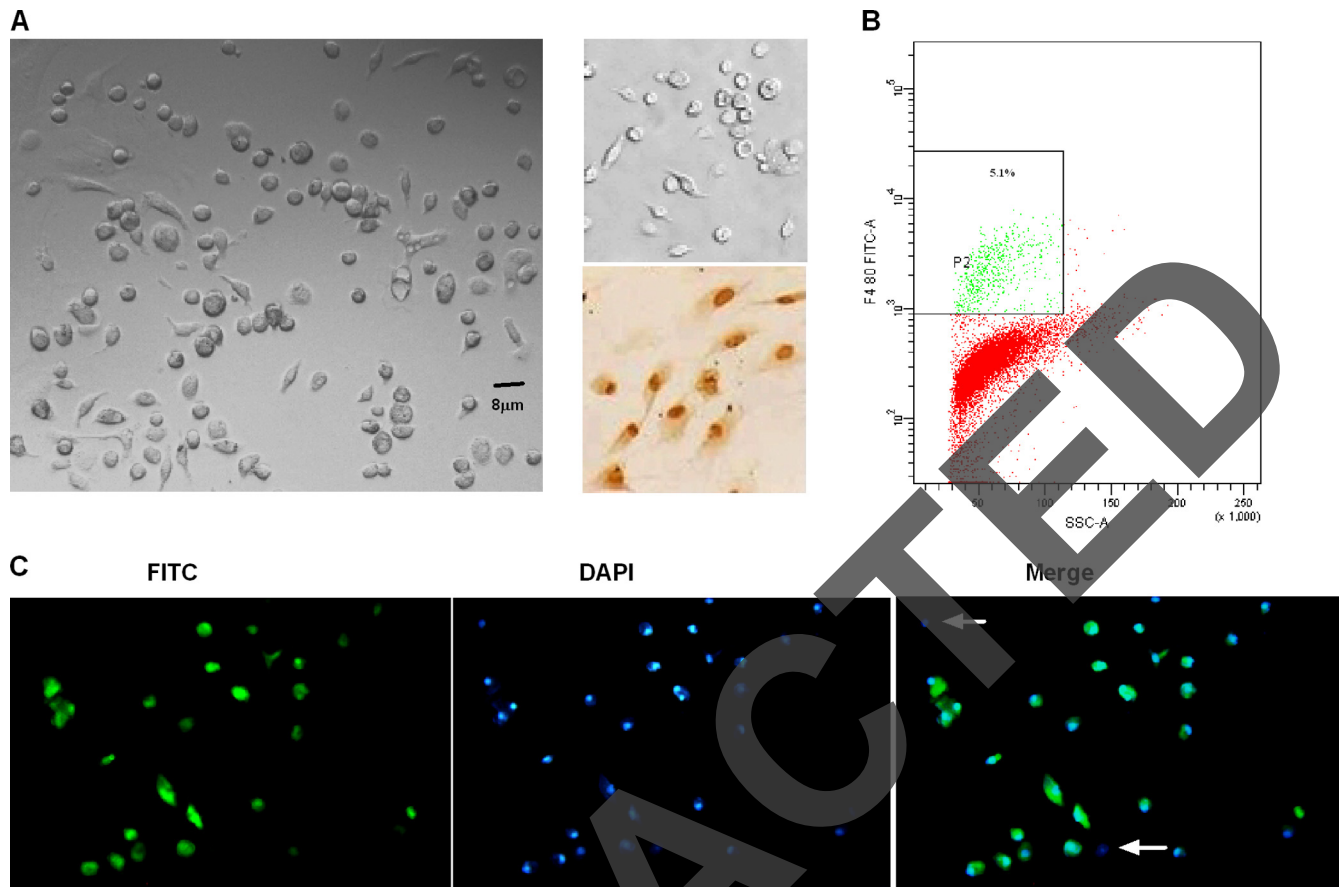
FIG 3 Identification of primary trophoblast cells. (A) The morphology and characterization of cultured cells are shown by inverted light microscopy in the left panel. In the upper right panel, primary cells on the coverslip were stained by immunoperoxidase with anti-vimentin-HRP. None of the analyzed samples reacted with anti-vimentin antibody. The positive control (NIH 3T3 cells, the mouse embryonic fibroblasts line) is shown in the lower right panel. (B) Anti-F4/80-FITC, one specific marker, was used to check the contamination of macrophage by FCM. (C) The phenotype and the purity of the isolated population were assessed by immunostaining for cytokeratin-7 (FITC; green). Cells are counterstained with 4′,6′-diamidino-2-phenylindole (DAPI; blue). Cells of negative reaction with cytokeratin-7 are rare (white arrow). The figure is representative of five independent experiments.

primary trophoblasts cocultured with *T. gondii* was also analyzed by FCM at different time intervals. We found that trophoblast apoptosis significantly increased after 12 h of coculture with *T. gondii* (Fig. 4C) compared with the control group.

T. gondii-induced trophoblast apoptosis is ROS dependent. To further confirm the role of ROS in *T. gondii*-triggered trophoblast apoptosis, *N*-acetylcysteine (Sigma, St. Louis, MO), a specific ROS quencher, was reconstituted in physiologic saline solution at a pH of 6.8 to 7.2 and administered at 100 mg/kg of body weight to the mice or at 10 μM to the primary cultured trophoblasts. From the analysis of TUNEL and FCM, we found that introduction of NAC significantly inhibited trophoblast apoptosis, not only in placental tissues (Fig. 5A and B) but also in primary cultured trophoblasts experimentally infected with *T. gondii* (Fig. 5C). Pretreatment with NAC decreased the apoptosis index of placental tissues compared with that of the infection group, especially in late apoptosis (Fig. 5B, right). Similar results were found in cocultured primary trophoblasts (from 41.3% to 27.6%) (Fig. 5C).

T. gondii-induced ROS initiates ERS response *in vivo*. Although overproduction of ROS can induce cell apoptosis via multiple pathways, such as MAPK or mitochondria, the endoplasmic reticulum may be more sensitive to oxidative stress. Therefore, we

observed the ERS markers in the placental tissues from each of the three groups. We found that these markers did not vary significantly across days of gestation in the control group (Fig. 6A), but there was a significant increase in caspase-12 and CHOP levels in the *T. gondii* infection group (Fig. 6B). To confirm the connection between ROS and increased levels of ERS markers, NAC was used in the antioxidant pretreatment group. We found that NAC treatment significantly inhibited the escalation of ERS molecules (Fig. 6C and D).

T. gondii infection contributes to apoptosis by activation of multiple proapoptotic pathways, including the ERS and ASK1/ JNK pathways. To observe the effect of *T. gondii*-triggered oxidative stress on endoplasmic reticulum and multiple proapoptotic pathways, a set of markers expressed during ER-induced apoptosis and UPR were checked by real-time PCR and immunoblotting. We found that the levels of major ERS markers, such as CHOP, GRP78, GRP94, and caspase-12, increased with *T. gondii* infection (Fig. 7A); compared to levels of GD10 in the control group, ASK1/ JNK and caspase-12 were significantly activated by phosphorylation or cleavage (Fig. 7B). However, the upregulation and activation of p38 were not observed in our data. In terms of these molecules, no significant difference was found in placental tissues
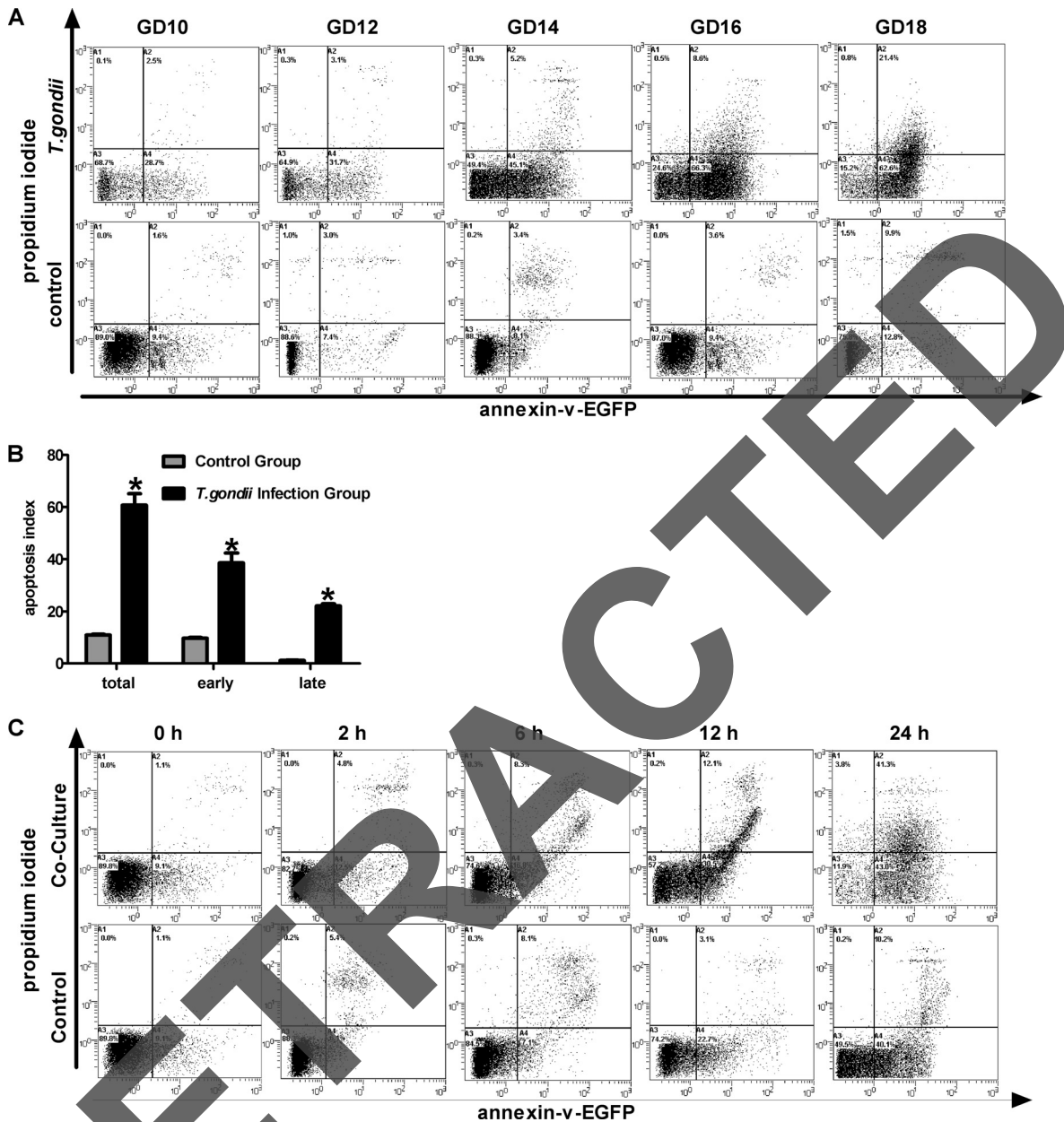
FIG 4 Effects of *T. gondii* infection on trophoblast apoptosis levels *in vitro* an *in vivo*. Freshly dissected placental tissues were processed into cell suspension, further labeled, and detected by FCM, as described in Materials and Methods. (A) *T. gondii* infection group and control group. (B) All samples at different days of pregnancy from the control group and the *T. gondii* infection group were reanalyzed by a Student's *t* test. *, $P < 0.001$ versus control. (C) Primary trophoblast culture and experimental infections were performed as described in the Materials and Methods. After challenge with *T. gondii* tachyzoites (parasite-to-cell ratio, 10^6:10^6), cells were harvested at 0, 2, 6, 12, and 24 h after coculture. Cells were treated according to the protocols, and treatment of the control group was performed simultaneously. The figure is representative of three independent experiments.

from the control groups across days of gestation (data not shown). The use of NAC significantly inhibited the upregulation and activation of these pathways, especially of the ERS markers, but not phosphorylation of JNK (Fig. 7C and D).

T. gondii induces production of ROS by increasing transcription of Nox1 mRNA in the early stage, followed by the exhaustion of GSH and activation of the ERS and the ASK1/JNK pathway. Nox1 is a key oxidase in the production of some oxide molecules. The upregulation of this oxidase in *T. gondii* infection was confirmed in this study (Fig. 1D). Members of the glutathione

peroxidase family are major antioxidant enzymes in mammals and catalyze the reduction of hydroxyperoxides by GSH. To investigate the mechanisms underlying ROS generation and the activation of the proapoptotic pathway, we detected the Nox1, Gpx1, and Gpx6 mRNA levels, the GSH protein level, and the activation of the ERS and ASK1/JNK pathways in one transwell cocultured system. Protein extraction and calculation of sample quantities in each lane were performed because the proportion of dead cells was increased after *T. gondii* infection. We found that Nox1 was upregulated first (Fig. 8A). Significantly elevated tran-
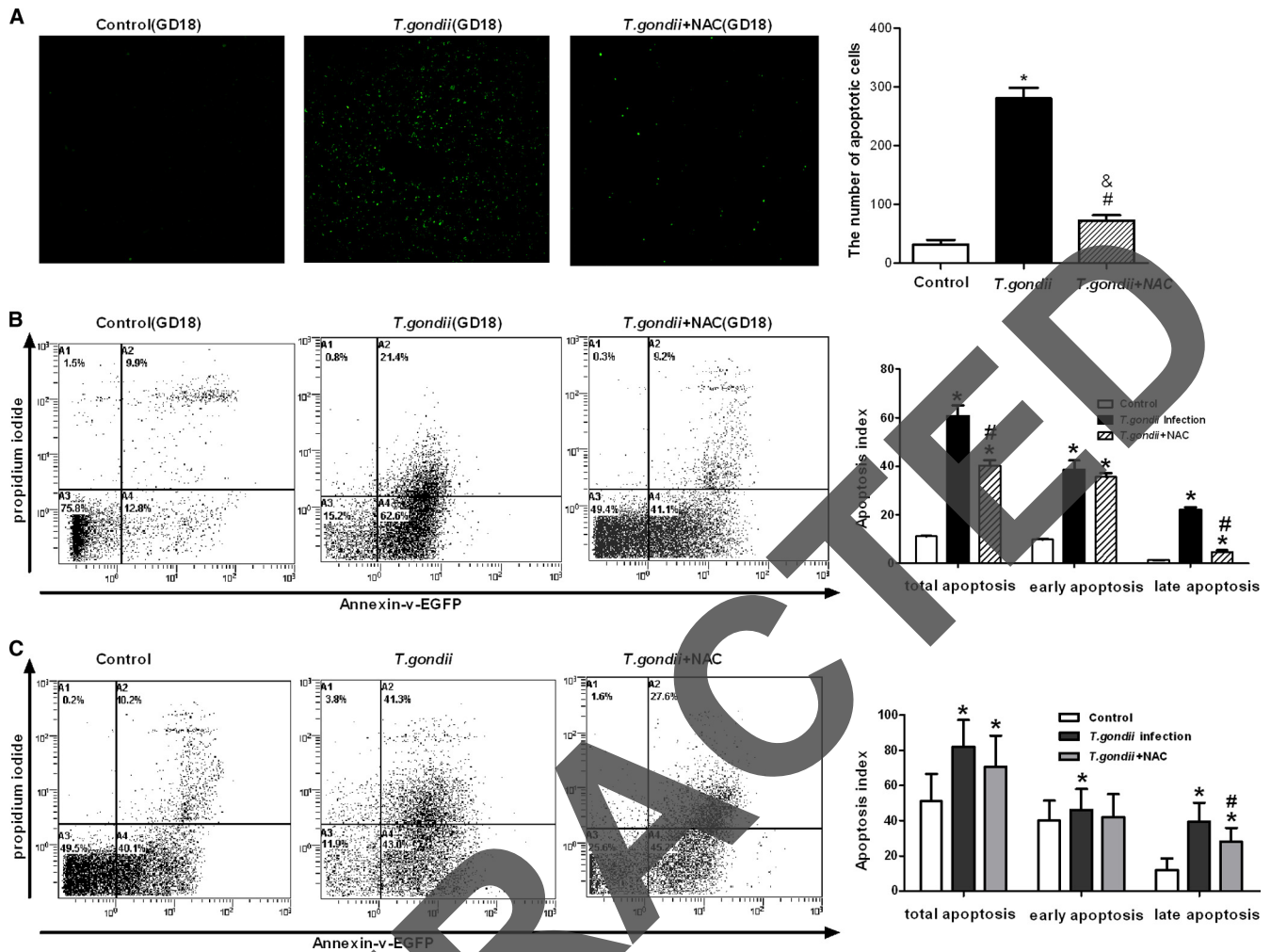
FIG 5 Effect of NAC on the apoptosis levels of placental tissues or primary cultured cells. (A) Apoptosis levels of placental tissues from GD18 were measured using a TUNEL assay, according to the manufacturer's instructions with some modifications. The results are shown as mean ± SD. The figure is representative of four independent experiments. (B) Cell suspensions from GD18 tissues from three groups were stained with EGFP-tagged annexin V and PI. The number in each quadrant represents the respective cell proportion. The figure is representative of six independent experiments. (C) Primary cells were divided into three groups: control, *T. gondii* infection, and NAC pretreatment. Primary cultured cells were harvested after coculture for 24 h, and the apoptosis levels were detected by FCM. The figure is representative of three independent experiments. #, $P < 0.01$ versus *T. gondii* infection; *, $P < 0.01$ versus the control; &, $P < 0.05$ versus the control.

scription of Gpx6 and Gpx1 mRNAs and a decrease in the GSH level were also detected after 6 h (Fig. 8A and B). From Western blot analysis, we found that GRP78 increased before other markers; then, the levels of CHOP and phosphorylation of JNK increased. Significantly increased phosphorylation of ASK1 and cleavage of caspase-12 were also observed after 6 h. However, p38 and phospho-p38 levels did not vary significantly across variable intervals (Fig. 8C). This observation could result from the limited observation period and lower pathogen load.

DISCUSSION

There is extensive evidence that oxidative stress or an imbalance between oxidant and antioxidant activity at the maternal-fetal interface plays a key role in the development of placenta-related diseases, including preeclampsia and miscarriage (28, 37). On the one hand, redox-sensitive signal transduction pathways are critical for developmental processes, including proliferation, differen-

tiation, and apoptosis of human tissues, especially for placenta; on the other hand, teratogens that induce oxidative stress, such as chemical poisoning and infection, may induce teratogenesis via the misregulation of the above-mentioned pathways (46). In particular, previous studies have discovered that ROS were involved in teratogenic processes in mice treated with LPS (7, 50), which is one well-recognized pathogen-associated molecular pattern (PAMP) of Gram-negative bacteria. Structures analogous to LPS have been found in *T. gondii*, such as glycosylphosphatidylinositols (GPI) (9, 36). Interestingly, all of these structures can trigger the activation of inflammatory cytokine expression by Toll-like receptor (TLR)-dependent pathways (25), e.g., TLR4 (10, 47) and TLR2 (6, 38). Some studies have revealed that LPS could induce the production of ROS in some organs, such as lung and liver (8, 51), in which ROS are important to the pathogenesis of organ damage (52).

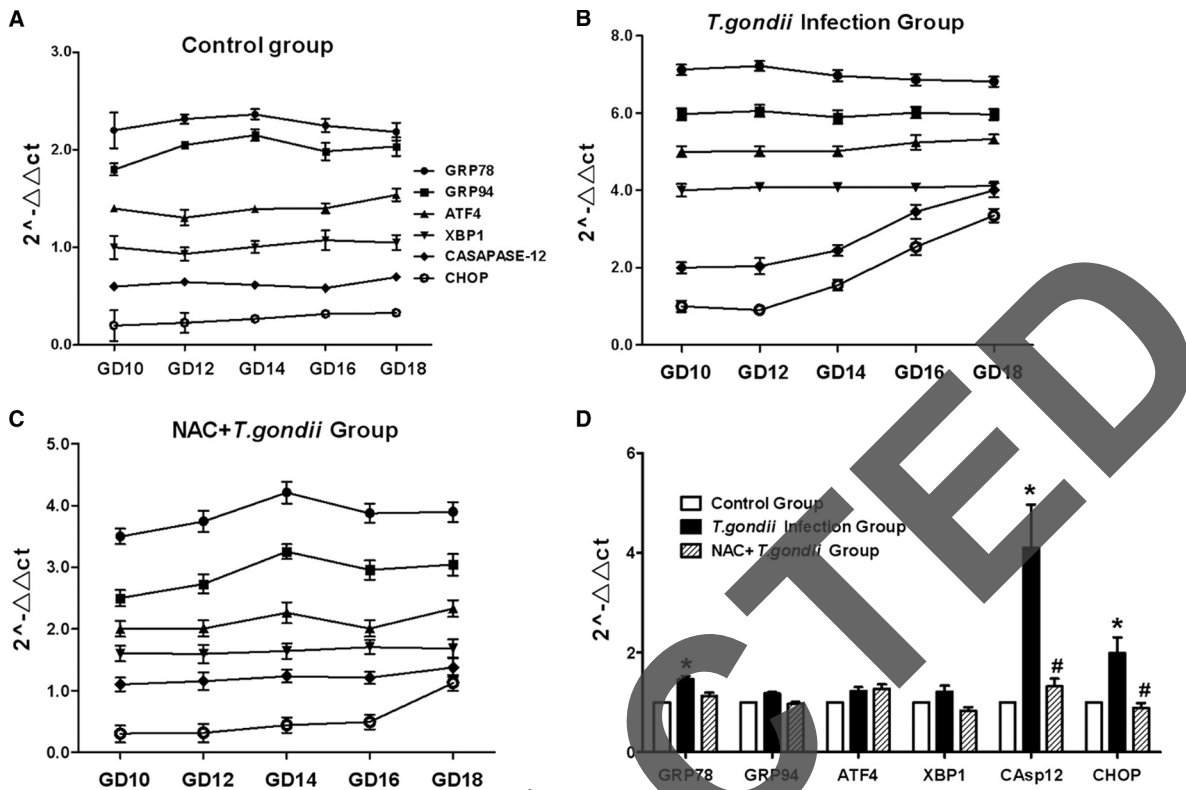In this study, we demonstrated that in mice, acute infection

FIG 6 ERS levels in placenta tissues of various gestational days from three groups. (A to C) The markers of ERS were detected by real-time RT-PCR in each group, as indicated. The data were normalized to those measured at GD10 in the same group. To prevent overlap, the data sets were moved by the same data units. (D) All samples across gestational days from the three groups were reanalyzed by one-way ANOVA and the SNK multiple comparison posttest. Values represent the mean ± SD of 30 samples per group. #, $P < 0.01$ versus *T. gondii* infection; *, $P < 0.01$ versus the control.

with RH tachyzoites (genotype I) in the second trimester contributed to the upregulation of a variety of oxide molecules and to an adaptive increase in the level of antioxidants in placental tissues. Oxidative stress was further confirmed by the decreased level of GSH and elevated levels of oxidation products (MDA and 8-OHdG) in placental tissues in the infection group. In addition to early decreased GSH, parasitemia was also found about 48 h after acute infection, followed by the abrupt increase of placental parasite burden on GD14. Therefore, based on our present study, oxidative stress caused by maternal infection, but not by placenta infection, may contribute to the structural damage to the placenta barrier in early stage, which benefited the invasion of *T. gondii*. Simultaneously, an increase in apoptosis of trophoblastic cells with *T. gondii* infection was observed by FCM and TUNEL *in vitro* and *in vivo*. Apoptosis levels increased with duration of infection but were not correlated with parasite burden.

In trophoblastic cells, apoptosis is a normal element of cell turnover, leading some cells to be eliminated without a local inflammatory reaction (19). *T. gondii*, however, is able to alter the apoptotic program of the host cells by promoting or inhibiting apoptosis (17). Previous studies have shown that modulation of apoptosis during *T. gondii* infection may be closely associated with the parasite's virulence factors (15), the state of infection of the individual cell (acute or chronic), the affected cell type, and the specific experimental conditions used. Apoptosis of bystander host cells may result from the secretion of some soluble factors by parasite-infected cells (31). In acute infection, major host tissue

cells could act as the bystanders, and lethal overproduction of Th1 cytokines may play an important role in pathogenesis (27). Here, we found increased trophoblast apoptosis, not only in placental tissues but also in primary cultured cells (mixed with immune cells), in the transwell coculture system. Our study reveals that elevated apoptosis does not result from direct physical damage but from the release of soluble factors. Additionally, we also found that pretreatment with antioxidants effectively suppressed local oxidative stress. GSH is a major intracellular antioxidant, and its biosynthesis depends on the intracellular availability of cysteine, which can be provided by *N*-acetylcysteine (NAC). The ameliorated redox condition in placental tissues resulted in a significant decrease in apoptosis, especially in late apoptosis. Similar results were obtained from the analysis of primary cultured trophoblasts in the coculture transwell system. Although in this study usage of antioxidant had a minor effect on early apoptosis, which could result from short-term usage of NAC, lower dosage, or factors other than ROS, existing data showed that acute *T. gondii* infection could induce cell apoptosis via oxidative stress, and ROS generation might be essential to this infection-mediated apoptosis.

ERS and oxidative stress are becoming increasingly recognized as inducers of pathological cell death leading to tissue dysfunction (22). ERS plays a critical role in the regulation of apoptosis caused by a variety of toxic insults that damage mammalian cells, including oxidative stress, hypoxia, chemicals, Ca^{2+}-homeostasis imbalance, and heavy metals (4, 26). Previous studies have revealed that the oxidative stress and ERS pathways are activated in the lungs of
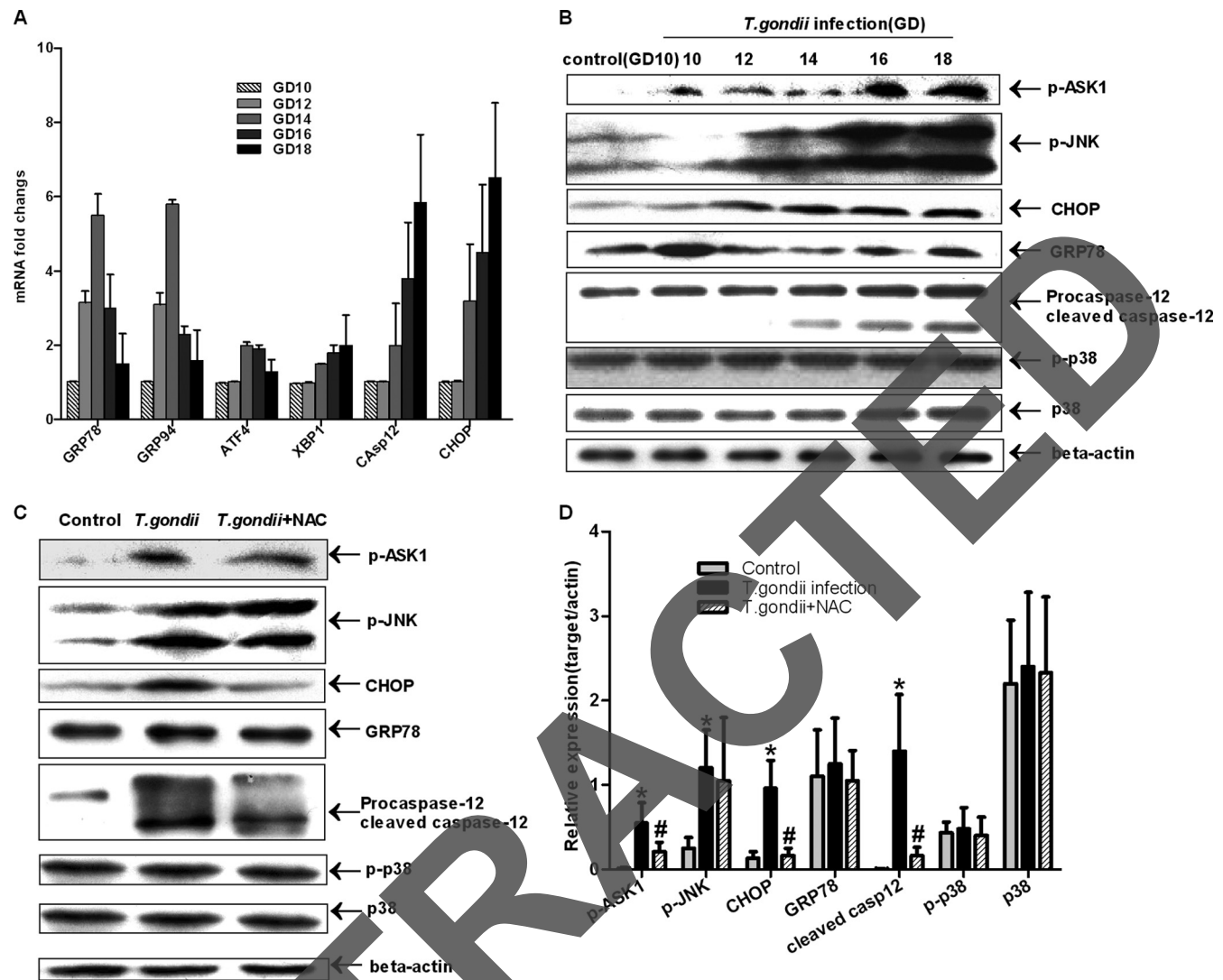
FIG 7 Activation of multiple proapoptotic pathways by *T. gondii* infection. (A) The data were normalized to the same gene, measured at GD10, in the control group. The data are means ± SDs and represent five independent experiments. Differences between gestational days were assessed by one-way ANOVA and the SNK multiple comparison posttest. (B) Placental cell lysates from different gestational days from the *T. gondii* infection group and GD10 from the control group were collected for immunoblotting with Abs against GRP78, CHOP, caspase-12, phospho-JNK (Thr183/Tyr185), phospho-ASK1 (Ser967), and total and phosphorylated (p-) forms of p38. β-Actin was used as an internal control. (C and D) Placental cell lysates of GD18 from three groups were checked by immunoblotting; a quantitative analysis of the Western blot analysis using densitometry (normalized to actin) is also shown. The figure is representative of five independent experiments. Values represent the mean ± SD of five samples in each group. #, $P < 0.01$ versus *T. gondii* infection; *, $P < 0.01$ versus the control.

LPS-treated mice (13, 43). Thus, we examined a number of ERS-related molecules and stress-activated signaling pathways, such as GRP78, CHOP, caspase-12, ASK1/JNK, and p38 cascades. The real-time RT-PCR revealed that GRP78, CHOP, and caspase-12 were upregulated in the *T. gondii* infection group. Western blotting of both *in vivo* and *in vitro* trophoblasts showed that the caspase-12 and ASK1/JNK cascades were activated and that caspase-12 was upregulated in infected mice in late pregnancy. Caspase-12 and CHOP are suspected to be specific to the apoptotic mechanism downstream of ERS because mice deficient in caspase-12 (29) and CHOP$^{-/-}$ cells (32) are resistant to ERS-mediated apoptosis. Previous reports showed that the activation of p38 and JNK was responsible for oxidative stress-induced apoptosis. Our study indicated that *T. gondii* infection might activate ASK1/JNK and that pretreatment with NAC significantly

inhibited phosphorylation of ASK1 rather than of JNK. No activation of p38 was seen in the present observation. Whether p38 is involved in this pathological process remains to be elucidated. The Nox4 isozyme is essential to LPS-induced production of ROS (33). By analysis of oxidative molecules in a coculture transwell system, we found that Nox1 was upregulated initially on challenge with *T. gondii* tachyzoites. Nox1 is a key oxidase in the production of some oxide molecules, such as superoxide anion and hydrogen peroxide. Additionally, a significant decrease in GSH, the most important antioxidant, was observed soon after Nox1 upregulation. These events finally triggered the endoplasmic reticulum response and inevitably induced trophoblast apoptosis. These results demonstrate that the oxidative response may be central to infection and the subsequent activation of those proapoptotic pathways.
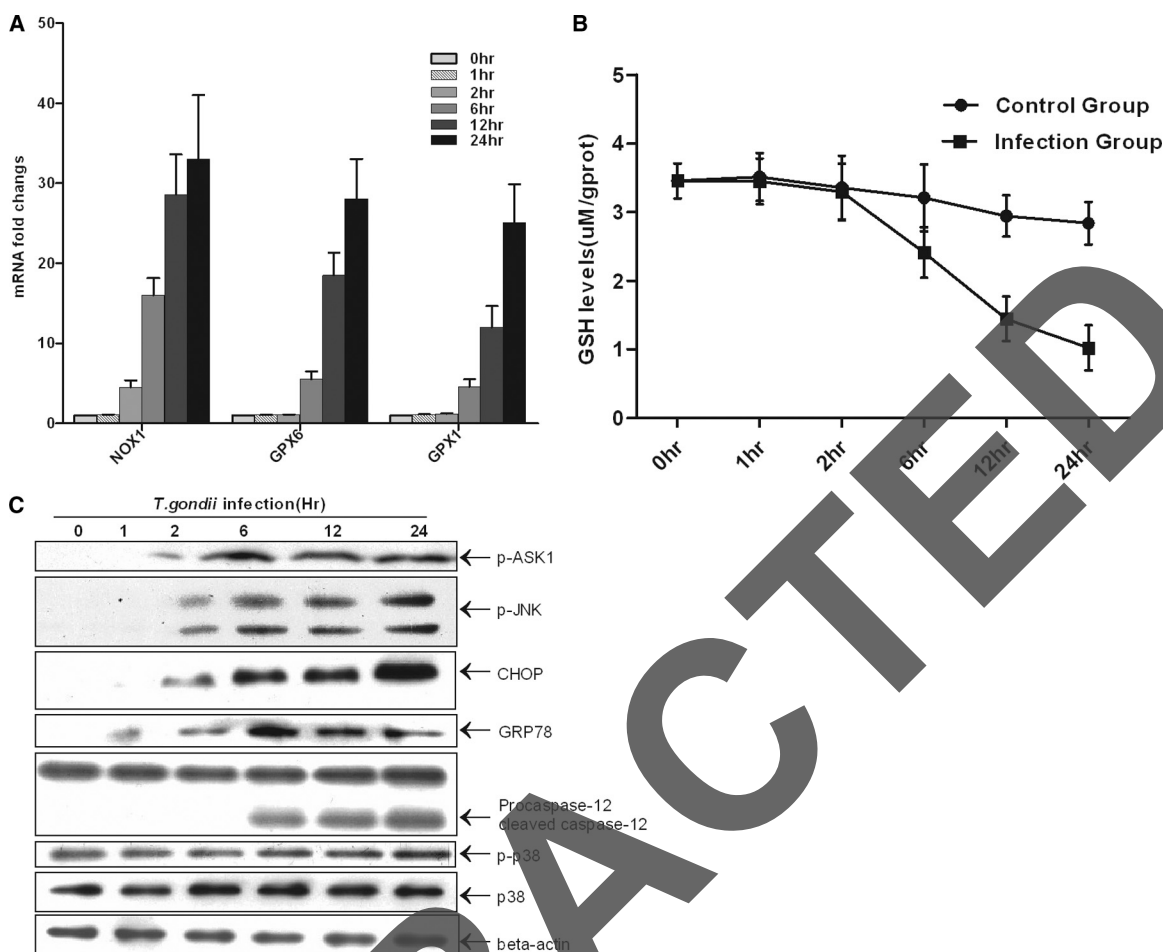
FIG 8 Induction of ROS and activation of the ERS pathway and ASK1/JNK by *T. gondii in vitro*. (A) Primary trophoblast cells were harvested after coculture for 0, 1, 2, 6, 12, and 24 h. RNA isolation and cDNA synthesis were performed per the conventional protocol. Quantitative real-time RT-PCR was conducted using the SYBR green method, and the mRNA fold induction values were calculated by the $2^{-\Delta\Delta CT}$ method. Data are means ± SDs of three independent experiments. (B) Primary cultured trophoblasts (10^6/well) were directly treated with 100 μl of lysis buffer. GSH was detected according to the manufacturer's instructions. Three independent experiments were conducted. (C) The trophoblast lysates experimentally infected by *T. gondii* were collected for immunoblotting.

In summary, from our present study, the increase of peroxidation products and apoptosis level of trophoblasts in placenta tissues was inconsistent with blood and placenta parasite burden but consistent with duration of infection. These data show that the intensity of the oxidative response at the maternal-fetal interface rather than the direct action of the parasite could account for different prognoses of infection. ROS-mediated ERS may partly contribute to cell apoptosis and pathophysiological injury induced by high-virulence *T. gondii*. These results are important to the understanding of the mechanisms underlying the process of pathological damage in *T. gondii* infection. Antioxidants have potential as a therapeutic regimen for the treatment of *T. gondii*-related diseases.

REFERENCES

1. **Abbasi M, et al.** 2003. Infection of placental trophoblasts by *Toxoplasma gondii*. J. Infect. Dis. **188**:608–616.

2. **Amarante-Paffaro A, Queiroz GS, Correa ST, Spira B, Bevilacqua E.** 2004. Phagocytosis as a potential mechanism for microbial defense of mouse placental trophoblast cells. Reproduction **128**:207–218.

3. **Barber EM, Fazzari M, Pollard JW.** 2005. Th1 cytokines are essential for placental immunity to *Listeria monocytogenes*. Infect. Immun. **73**:6322–6331.

4. **Biagioli M, et al.** 2008. Endoplasmic reticulum stress and alteration in calcium homeostasis are involved in cadmium-induced apoptosis. Cell Calcium **43**:184–195.

5. **Burton GJ, Yung HW, Cindrova-Davies T, Charnock-Jones DS.** 2009. Placental endoplasmic reticulum stress and oxidative stress in the pathophysiology of unexplained intrauterine growth restriction and early onset preeclampsia. Placenta **30**(Suppl A):S43–S48.

6. **Campos MA, et al.** 2001. Activation of Toll-like receptor-2 by glycosylphosphatidylinositol anchors from a protozoan parasite. J. Immunol. **167**:416–423.

7. **Carey LC, Berbee PL, Coyle P, Philcox JC, Rofe AM.** 2003. Zinc treatment prevents lipopolysaccharide-induced teratogenicity in mice. Birth Defects Res. A Clin. Mol. Teratol. **67**:240–245.

8. **da Cunha AA, et al.** 2011. Treatment with N-methyl-D-aspartate receptor antagonist (MK-801) protects against oxidative stress in lipopolysaccharide-induced acute lung injury in the rat. Int. Immunopharmacol. **11**:706–711.

9. **Debierre-Grockiego F, et al.** 2003. Roles of glycosylphosphatidylinositols of *Toxoplasma gondii*. Induction of tumor necrosis factor-alpha production in macrophages. J. Biol. Chem. **278**:32987–32993.

10. **Debierre-Grockiego F, et al.** 2007. Activation of TLR2 and TLR4 by glycosylphosphatidylinositols derived from *Toxoplasma gondii*. J. Immunol. **179**:1129–1137.

11. **Ding SZ, et al.** 2007. *Helicobacter pylori* infection induces oxidative stress and programmed cell death in human gastric epithelial cells. Infect. Immun. **75**:4030–4039.

12. **Elsheikha HM, El-Motayam MH, Abouel-Nour MF, Morsy AT.** 2009. Oxidative stress and immune-suppression in *Toxoplasma gondii* positive blood donors: implications for safe blood transfusion. J. Egypt Soc. Parasitol. **39**:421–428.

13. **Endo M, Oyadomari S, Suga M, Mori M, Gotoh T.** 2005. The ER stress pathway involving CHOP is activated in the lungs of LPS-treated mice. J. Biochem. **138**:501–507.

14. **Fang Y, Yu S, Ellis JS, Sharav T, Braley-Mullen H.** 2010. Comparison of sensitivity of Th1, Th2, and Th17 cells to Fas-mediated apoptosis. J. Leukoc. Biol. **87**:1019–1028.

15. **Gavrilescu LC, Denkers EY.** 2001. IFN-γ Overproduction and high level apoptosis are associated with high but not low virulence *Toxoplasma gondii* Infection. J. Immunol. **167**:902–909.

16. **Geva E, et al.** 2002. Human placental vascular development: vasculogenic and angiogenic (branching and nonbranching) transformation is regulated by vascular endothelial growth factor-A, angiopoietin-1, and angiopoietin-2. J. Clin. Endocrinol. Metab. **87**:4213–4224.

17. **Heussler VT, Kuenzi P, Rottenberg S.** 2001. Inhibition of apoptosis by intracellular protozoan parasites. Int. J. Parasitol. **31**:1166–1176.

18. **Hoshida MS, et al.** 2007. Regulation of gene expression in mouse trophoblast cells by interferon-gamma. Placenta **28**:1059–1072.

19. **Huppertz B, Kadyrov M, Kingdom JC.** 2006. Apoptosis and its role in the trophoblast. Am. J. Obstet. Gynecol. **195**:29–39.

20. **Jauniaux E, et al.** 2000. Onset of maternal arterial blood flow and placental oxidative stress. A possible factor in human early pregnancy failure. Am. J. Pathol. **157**:2111–2122.

21. **Kaneto H, et al.** 2005. Oxidative stress, ER stress, and the JNK pathway in type 2 diabetes. J. Mol. Med. **83**:429–439.

22. **Kim I, Xu W, Reed JC.** 2008. Cell death and endoplasmic reticulum stress: disease relevance and therapeutic opportunities. Nat. Rev. Drug Discov. **7**:1013–1030.

23. **Kim WH, et al.** 2010. Suppression of CD4 T-Cells in the spleen of mice infected with Toxoplasma gondii KI-1 tachyzoites. Korean J. Parasitol. **48**:325–329.

24. **Kitamura M, Hiramatsu N.** 2010. The oxidative stress: endoplasmic reticulum stress axis in cadmium toxicity. Biometals **23**:941–950.

25. **Krishnegowda G, et al.** 2005. Induction of proinflammatory responses in macrophages by the glycosylphosphatidylinositols of *Plasmodium falciparum*: cell signaling receptors, glycosylphosphatidylinositol (GPI) structural requirement, and regulation of GPI activity. J. Biol. Chem. **280**:8606–8616.

26. **Kubota K, et al.** 2005. Fluoride induces endoplasmic reticulum stress in ameloblasts responsible for dental enamel formation. J. Biol. Chem. **280**:23194–23202.

27. **Mordue DG, Monroy F, La Regina M, Dinarello CA, Sibley LD.** 2001. Acute toxoplasmosis leads to lethal overproduction of Th1 cytokines. J. Immunol. **167**:4574–4584.

28. **Myatt L, Cui X.** 2004. Oxidative stress in the placenta. Histochem. Cell Biol. **122**:369–382.

29. **Nakagawa T, et al.** 2000. Caspase-12 mediates endoplasmic-reticulum-specific apoptosis and cytotoxicity by amyloid-beta. Nature **403**:98–103.

30. **Nakka VP, Gusain A, Raghubir R.** 2010. Endoplasmic reticulum stress plays critical role in brain damage after cerebral ischemia/reperfusion in rats. Neurotox. Res. **17**:189–202.

31. **Nishikawa Y, et al.** 2007. *Toxoplasma gondii* infection induces apoptosis in noninfected macrophages: role of nitric oxide and other soluble factors. Parasite Immunol. **29**:375–385.

32. **Oyadomari S, Araki E, Mori M.** 2002. Endoplasmic reticulum stress-mediated apoptosis in pancreatic beta-cells. Apoptosis **7**:335–345.

33. **Park HS, et al.** 2004. Cutting edge: direct interaction of TLR4 with NAD(P)H oxidase 4 isozyme is essential for lipopolysaccharide-induced production of reactive oxygen species and activation of NF-κB. J. Immunol. **173**:3589–3593.

34. **Payne TM, Molestina RE, Sinai AP.** 2003. Inhibition of caspase activation and a requirement for NF-κB function in the *Toxoplasma gondii*-mediated blockade of host apoptosis. J. Cell Sci. **116**:4345–4358.

35. **Pfaff AW, et al.** 2007. Cellular and molecular physiopathology of congenital toxoplasmosis: the dual role of IFN-gamma. Parasitology **134**:1895–1902.

36. **Pollard AM, Onatolu KN, Hiller L, Haldar K, Knoll LJ.** 2008. Highly polymorphic family of glycosylphosphatidylinositol-anchored surface antigens with evidence of developmental regulation in *Toxoplasma gondii*. Infect. Immun. **76**:103–110.

37. **Redman CW, Sargent IL.** 2005. Latest advances in understanding preeclampsia. Science **308**:1592–1594.

38. **Ronnberg E, Guss B, Pejler G.** 2010. Infection of mast cells with live streptococci causes a toll-like receptor 2- and cell-cell contact-dependent cytokine and chemokine response. Infect. Immun. **78**:854–864.

39. **Senegas A, et al.** 2009. *Toxoplasma gondii*-induced foetal resorption in mice involves interferon-gamma-induced apoptosis and spiral artery dilation at the maternofoetal interface. Int. J. Parasitol. **39**:481–487.

40. **Sener G, et al.** 2006. Melatonin prevents neutrophil-mediated oxidative injury in *Escherichia coli*-induced pyelonephritis in rats. J. Pineal Res. **41**:220–227.

41. **Siemieniuk E, Kolodziejczyk L, Skrzydlewska E.** 2008. Oxidative modifications of rat liver cell components during *Fasciola hepatica* infection. Toxicol. Mech. Methods **18**:519–524.

42. **Tenter AM, Heckeroth AR, Weiss LM.** 2000. Toxoplasma gondii: from animals to humans. Int. J. Parasitol. **30**:1217–1258.

43. **Valenca SS, et al.** 2008. Oxidative stress in mouse plasma and lungs induced by cigarette smoke and lipopolysaccharide. Environ. Res. **108**:199–204.

44. **Wang H, Hirsch E.** 2003. Bacterially-induced preterm labor and regulation of prostaglandin-metabolizing enzyme expression in mice: the role of Toll-like receptor 4. Biol. Reprod. **69**:1957–1963.

45. **Watson D, Loweth AC.** 2009. Oxidative and nitrosative stress in beta-cell apoptosis: their contribution to beta-cell loss in type 1 diabetes mellitus. Br. J. Biomed. Sci. **66**:208–215.

46. **Wells PG, et al.** 2009. Oxidative stress in developmental origins of disease: teratogenesis, neurodevelopmental deficits, and cancer. Toxicol. Sci. **108**:4–18.

47. **Whitaker SM, Colmenares M, Pestana KG, McMahon-Pratt D.** 2008. *Leishmania pifanoi* proteoglycolipid complex P8 induces macrophage cytokine production through Toll-like receptor 4. Infect. Immun. **76**:2149–2156.

48. **Yang P, Zhao Z, Reece EA.** 2008. Activation of oxidative stress signaling that is implicated in apoptosis with a mouse model of diabetic embryopathy. Am. J. Obstet. Gynecol. **198**:130.e1-130.e7.

49. **Yavuz E, et al.** 2006. *Granulomatous villitis* formed by inflammatory cells with maternal origin: a rare manifestation type of placental toxoplasmosis. Placenta **27**:780–782.

50. **Zhao L, et al.** 2008. Reactive oxygen species contribute to lipopolysaccharide-induced teratogenesis in mice. Toxicol. Sci. **103**:149–157.

51. **Zhu JH, Lei XG.** 2011. Lipopolysaccharide-induced hepatic oxidative injury is not potentiated by knockout of GPX1 and SOD1 in mice. Biochem. Biophys. Res. Commun. **404**:559–563.

52. **Zou W, Roth RA, Younis HS, Burgoon LD, Ganey PE.** 2010. Oxidative stress is important in the pathogenesis of liver injury induced by sulindac and lipopolysaccharide cotreatment. Toxicology **272**:32–38.